Kinetic Study on the Poly(methyl methacrylate) Seeded Soapless Emulsion Polymerization of Styrene. II. Kinetic Model

CHIA-FEN LEE,[1] WEN-YEN CHIU,[2,*] and YUAN-CHEN CHERN[2]

[1]Institute of Materials Science and Engineering, and [2]Department of Chemical Engineering, National Taiwan University, Taipei, Taiwan, Republic of China

SYNOPSIS

A seeded soapless emulsion polymerization was carried out with poly(methyl methacrylate) (PMMA) as seeds, styrene as monomers, and potassium persulfate ($K_2S_2O_8$) as the initiator to synthesize the PMMA/polystyrene (PS) composite latex. The morphology of the latex particles was observed by transmission electron microscopy (TEM). It showed a core–shell structure. A core–shell kinetic model was proposed for the seeded emusion polymerization, in which the thickness of the shell was not constant. An increase of the conversion would increase the thickness of the shell. The entire course of polymerization could be divided into three regions: In the first region, the propagation rate constant (K_p) and termination rate constant (K_t) were kept constant at constant temperature. The kinetic data showed that the square root of polymer yield ($W_p^{1/2}$) was proportional to the reaction time. In the second region, the gel effect was considered and the termination rate constant (K_t) was empirically modified. The K_t would decrease with increasing the conversion. In the third region, both the gel effect and the glassy effect were considered; the propagation rate constant was also empirically modified. The prediction on the conversion and the number-average molecular weight of polymers during the seeded emusion of polymerization on the basis of our core–shell kinetic model fitted well with the experimental data. © 1995 John Wiley & Sons, Inc.

INTRODUCTION

In our previous work,[1] a seeded emulsion polymerization (or two-stage emulsion polymerization) was used to synthesize core–shell polymer/polymer composites. In seeded emulsion polymerization,[2-7] usually no new particles formed during the polymerization reaction. The seed particles would continuously grow with the reaction. The mechanism and kinetics on the growth of polymer particles have been studied by a number of workers in recent years. In 1970, Grancio and Williams[8] pointed out that the monomers distributed in the polymer particle were not uniform. They created a core–shell model in that the polymer core was surrounded by a layer of the monomer shell. The monomer shell was the reaction zone, and the thickness of the shell was constant. In 1971, Wessling and Harrison[9] created the surface polymerization model. In 1976, Ugelstad and Hansen[10] applied the Smith–Ewart model (case III) to the core–shell model. Their model pointed out that the core was only a polymer and the shell was a mixing solution of polymer and monomer. The shell was the reaction zone, and in the entire curve of polymerization, the thickness of the shell was kept constant. The prediction of kinetic data from the model showed that the $\frac{2}{3}$ power of the polymer yield was proportional to the reaction time. In 1979, Gardon[11] pointed out that the monomers were distributed in the polymer particles uniformly, and before monomer droplets disappeared, the number of free radicals in the polymer particle was not constant.

So far, there have been few articles dealing with the synthesis of composite latex by the method of soapless emulsion polymerization. In this work, no emulsifier was added in our seeded emulsion poly-

* To whom correspondence should be addressed.

Journal of Applied Polymer Science, Vol. 57, 591–603 (1995)
 CCC 0021-8995/95/050591-13

merization. The purpose of the present study was to investigate the mechanism of the soapless seeded emulsion polymerization, in which the composite polymer particles were with a core–shell structure. A new core–shell kinetic model was proposed to predict the conversion and the number-average molecular weight of polymers during the seeded emulsion polymerization.

EXPERIMENTAL

Materials

Methyl methacrylate and styrene were distilled under nitrogen atmosphere and reduced pressure prior to polymerization. Water was redistilled and deionized. Other chemicals were of analytical grade and used without further purification.

Polymerization

Two-stage polymerization reactions were carried out with the detailed procedures mentioned in Part I of our work. The first stage was to synthesize the PMMA seed latex; the ingredients and conditions for polymerization were shown in Table 1 in Part I of our work. After the reaction of first stage was complete, quantitative styrene and $K_2S_2O_8$ were added into the seed latex, and the reaction of the second stage began. The ingredient and conditions for the second-stage polymerization were shown in Table 2 in Part I of our work.

Conversion

The monomer conversion was determined gravimetrically. The detailed method and the calculation of conversion were stated in Part I of our work.

Particle Size and Size Distribution

The particle size and size distribution were measured by TEM. The detailed method was stated in Part I of our work.

Molecular Weight Determination

The number-average molecular weight of the polymers was determined with a Shodex RI gel permeation chromatograph (GPC Model SE-61) on dry samples dissolved in tetrahydrofuran. In the seeded polymerization, the polymer that we obtained contained both poly(methyl methacrylate) (PMMA) and polystyrene (PS), so a mixed Q factor used in our calculation of GPC curve was required. The method of calculation was stated in Part I of our work, and the mixed Q factor was defined in Part I as

$$\frac{1}{Q_{\text{mix}}} = \frac{W_{\text{PMMA}}}{Q_{\text{PMMA}}} + \frac{W_{\text{PS}}}{Q_{\text{PS}}}$$

where W_{PMMA} is the weight fraction of PMMA in the mixture of PMMA and PS; W_{PS}, the weight fraction of PS in the mixture of PMMA and PS; Q_{PMMA}, the Q factor of PMMA; and Q_{PS}, the Q factor of PS.

Observation of Particle Morphology

The latex particles from the seeded polymerization were ultramicrotomed and stained with RuO_4. The stained sections of the latex particles were observed under the transmission electron microscope (TEM).

Concentration of Styrene in PS Latex

The PS latex was prepared by soapless emulsion polymerization of styrene;[12] then, the PS latex emulsion was quenched to room temperature. Quantitative styrene was added into the PS latex emulsion and stirred at room temperation for 24 h. The concentration of styrene in PS latex was measured by the method stated in the Experimental subsection "Concentration of Monomer in Polymer Particles" in Part I of our work.

Concentration of Styrene in PMMA Latex

The PMMA latex was prepared by soapless emulsion polymerization of MMA. Styrene was then added into the PMMA latex. The concentration of styrene in PMMA later was determined by the same method stated above in Concentration of Styrene in PS Latex.

THEORETICAL CONSIDERATION

Core–Shell Model

A core–shell kinetic model was proposed for the polymerization of styrene in polymer particles. In our soapless seeded emulsion polymerization system, i.e., the polymerization of styrene with PMMA as seeds, the PS polymer chains were initiated by $K_2S_2O_8$ and the functional group (SO_4—) at the end of polymer chains was hydrophilic, but the polymer chains were hydrophobic. So, the hydrophilic group SO_4—

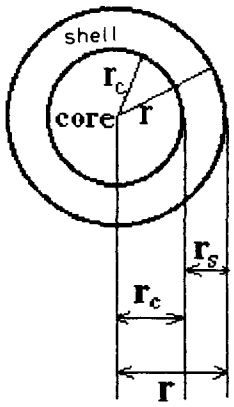

Figure 1 A polymer particle with core and shell regions.

would anchor on the surface of the polymer particles, assuming that the monomer was distributed in the polymer particles uniformly,[11] but that the reaction loci were on the surface layer. When the system still had monomer droplets, the concentration of the monomer in the polymer particles was retained at saturated concentration. That was because monomers would diffuse quickly from droplets to polymer particles for the reaction of polymerization. But when the monomer droplets disappeared, the monomers inside the polymer particles had to diffuse outward to the surface layer for the reaction of polymerization. Because the T_g of PMMA (about 120°C) was higher than was the reaction temperature (60 or 70°C), it was difficult for PMMA to diffuse outside. The mechanism described above resulted in the core–shell morphology of polymer particles.

Figure 1 shows the core and the shell regions in the one-polymer particle; the core region was PMMA seed swollen with styrene. The shell region was the reaction zone, containing styrene and PS formed from the reaction of polymerization.

During polymerization, the thickness of the reaction zone (r_s) or the volume of the reaction zone increased with increasing the conversion. The styrene monomer was assumed to be uniformly distributed in either the core or shell region of the polymer particles.

From the mass balance of the styrene monomer, we obtained

$$\tfrac{4}{3}\pi r_c^3[M]_c + [M]_s[\tfrac{4}{3}\pi(r^3 - r_c^3)] = \tfrac{4}{3}\pi r^3[M]_p \quad (1)$$

where $[M]_c$ is the monomer concentration in the core (mol/L); $[M]_s$, the monomer concentration in the shell (mol/L); and $[M]_p$, the average monomer concentration in the polymer particle (mol/L).

Another independent experiment showed that the saturated concentration of styrene in the PS latex

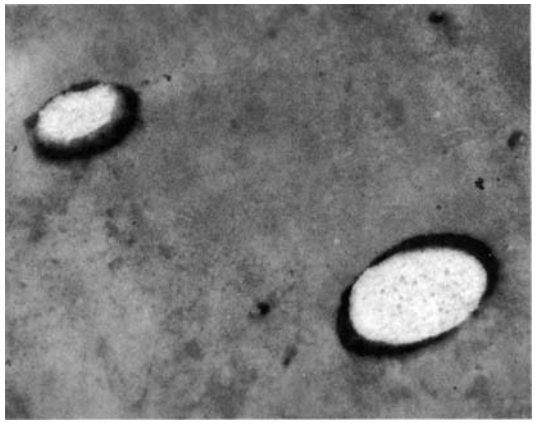

Figure 2 TEM photograph (magnification = 75 K) of sectioned polymer particles at the end of the second-stage reaction; seed latex = 49.18 g; $K_2S_2O_8$ = 0.855 g; T = 70°C; styrene = 73.77 g; MMA/ST = 1/1.5.

was the same as that in the PMMA latex; the concentration was about 3 mol/L at room temperature. In addition, the solubility parameters of PS and PMMA were very alike,[13] so the value of $[M]_s$ was assumed to be equal to the value of $[M]_c$ in our model

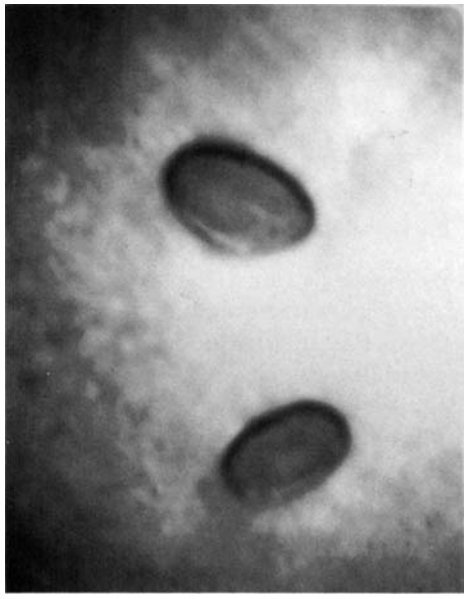

Figure 3 TEM photograph (magnification = 75 K) of sectioned polymer particles at the end of the second-stage reaction, seed latex = 49.18 g; AIBN = 0.5 g; T = 70°C; styrene = 24.59 g; MMA/ST = 1/0.5.

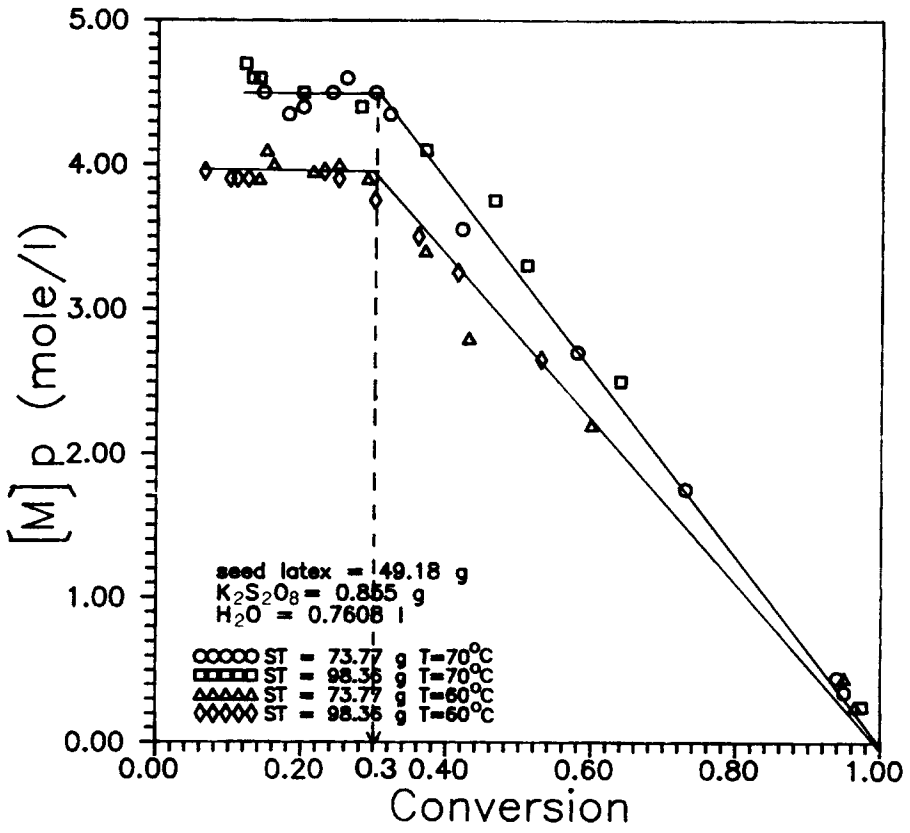

Figure 4 Concentration of monomer in polymer particles vs. conversion.

for the system of the PMMA/PS composite latex. Introducing the relation of $[M]_s = [M]_c$ into eq. (1), we obtained

$$[M]_s = [M]_c = [M]_p \tag{2}$$

Rate of Polymerization

In our soapless seeded emulsion polymerization, the system contained a fixed number of polymer particles. Refer to Part I, Figure 4, the distribution of polymer particles was observed under the TEM. It showed that the particles were always of uniform size over the entire course of polymerization. Therefore, it could be concluded that no new particles formed during the second-stage polymerization.

Each particle was with the core–shell structure as seen in Figure 1. The shell was the reaction zone, i.e., the polymerization reaction took place only on the shell. Then, the rate of polymerization could be expressed as

$$R_p = K_p[M]_s[R\cdot]V_rN \tag{3}$$

where R_p is the rate of polymerization; K_p, the propagation rate constant; $[M]_s$, the monomer concentration in the shell; $[R\cdot]$, the concentration of radicals in the one-polymer particle; V_r, the volume of the reaction zone in the one-polymer particle; and N, the number of polymer particles per unit volume of water.

Assuming the steady state for all radicals:

$$\rho_i = R_t = K_t[R\cdot]^2V_rN \tag{4}$$

where ρ_i is the generation rate of radicals; R_t, the termination rate of radicals; and K_t, the termination rate constant, then

$$[R\cdot] = \left(\frac{\rho_i}{K_tV_rN}\right)^{1/2} \tag{5}$$

and the rate of polymerization, R_p, is expressed as

$$R_P = K_P[M]_S\left(\frac{\rho_i}{K_tV_rN}\right)^{1/2}V_rN$$

$$= K_P[M]_s\left(\frac{\rho_iN}{K_t}\right)^{1/2}V_r^{1/2} \tag{6}$$

In the reaction zone of the polymer particles, the monomer content was determined from the concen-

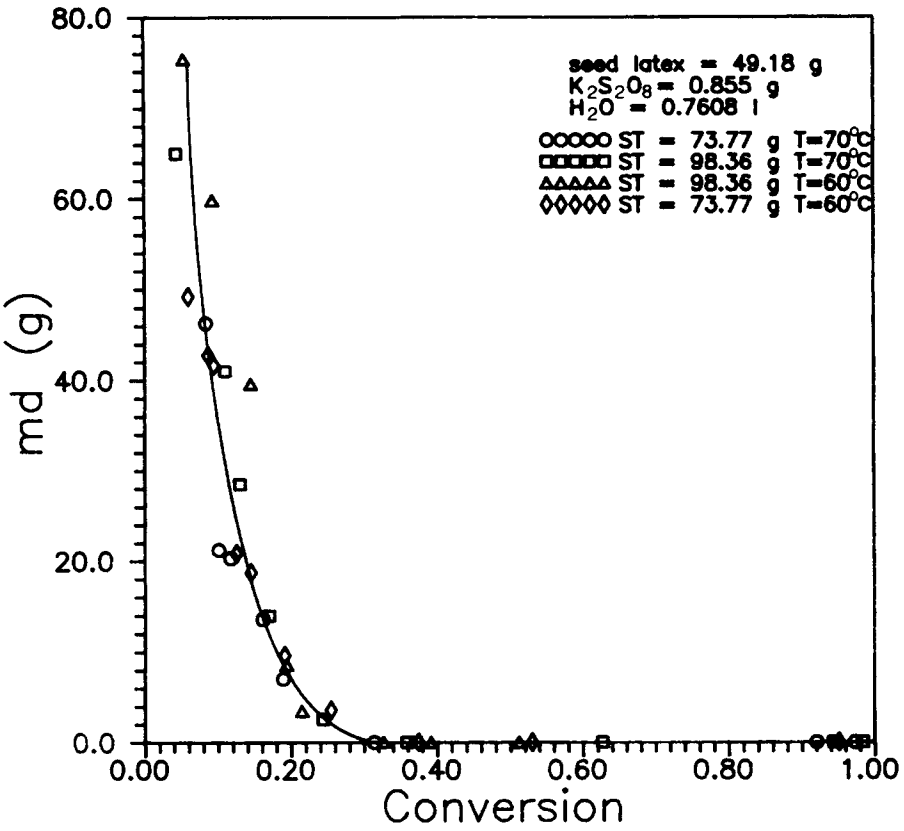

Figure 5 Weight of monomer droplets in system vs. conversion.

tration of styrene in the shell ($[M]_s$), and the polymer content was determined from the yield of PS (W_p). The total volume of the monomer and polymer in the reaction zone was calculated simply by the additivity rule as follows:

$$V_r = \frac{W_P}{\rho_p N} + \frac{[M]_s V_r \cdot 104}{\rho_M} \tag{7}$$

$$\Rightarrow V_r = \frac{W_p}{\rho_p\left(1 - \dfrac{[M]_s \cdot 104}{\rho_M}\right)N} \tag{8}$$

where W_p is the polymer (PS) yield (grams per liter of water) in the seeded polymerization; ρ_p, the density of the polymer (PS); ρ_M, the density of the styrene monomer; and 104, the molecular weight of the styrene monomer. Substituting V_r into R_p, we obtained

$$R_P = K_P[M]_S\left(\frac{\rho_i}{K_t}\right)^{1/2} \frac{W_p^{1/2}}{\rho_p^{1/2}\left(1 - \dfrac{[M]_S \cdot 104}{\rho_M}\right)^{1/2}} \tag{9}$$

Three regions were considered over the entire course of polymerization:

Region I ***($0 \leq x < x_c$)***

Before the monomer droplets disappeared, $[M]_s$ (or $[M]_p$) was kept constant. In this region, $[M]_p$ was equal to the saturated monomer concentration in polymer particles ($[M]_g$).

The half-life of $K_2S_2O_8$ was very long, so the concentration of the initiator was assumed to be constant over the polymerization, i.e.:

$$\rho_i = 2kdf[I] = \text{constant} \tag{10}$$

where k_d is the rate constant for the initiator decomposition; f, the initiator efficiency; and $[I]$, the initiator concentration. From the relation of R_p to x, and W_p to x,

$$R_p = [M]_0 \frac{dx}{dt}$$

i.e., (11)

$$W_p = x \cdot 104[M]_0$$

where $[M]_0$ is the initial concentration of the monomer in the system.

Equation (9) can be rewritten as

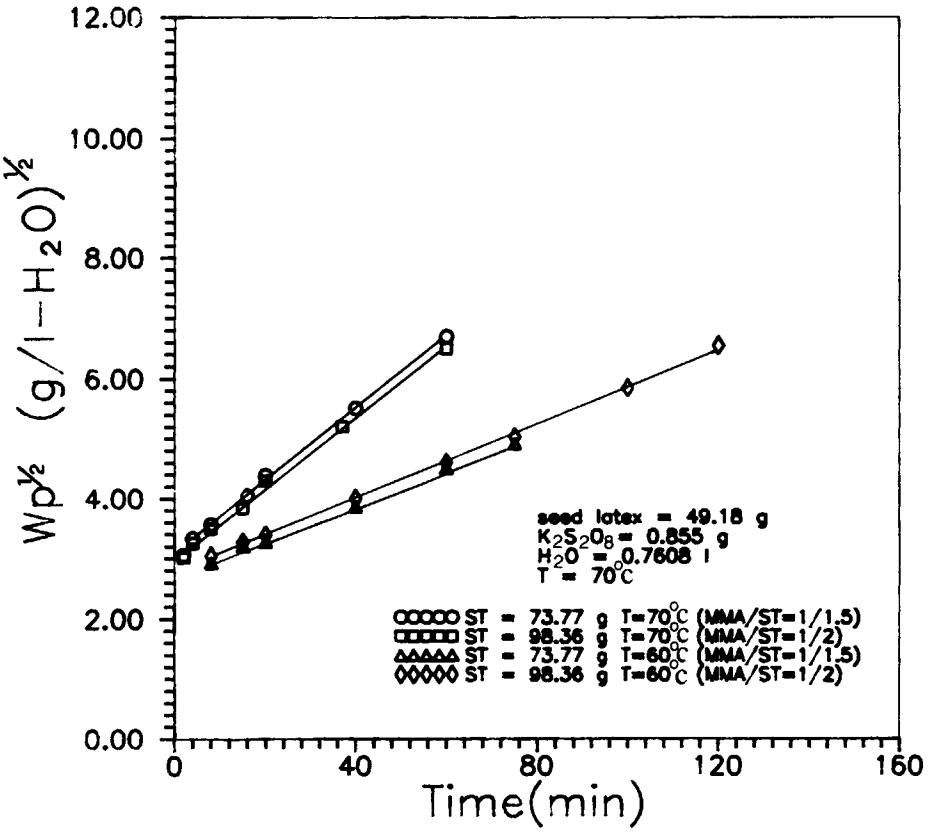

Figure 6 $W_p^{1/2}$ vs. reaction time.

$$\frac{dx}{dt} = K_{P_0}[M]_g \times \left(\frac{\rho_i}{K_{t_0}}\right)^{1/2}\left(\frac{x \cdot 104}{[M]_0\rho_p\left(1 - \dfrac{[M]_g \cdot 104}{\rho_M}\right)}\right)^{1/2} \quad (12)$$

or

$$\frac{W_p^{1/2} - W_{p_0}^{1/2}}{t - t_0} = K_{P_0}[M]_g\left(\frac{\rho_i}{K_{t_0}\rho_p}\right)^{1/2} \frac{52}{\left(1 - \dfrac{[M]_g \cdot 104}{\rho_M}\right)^{1/2}} \quad (13)$$

where W_{p_0} is the PS yield initially ($t = t_0 = 0$) in the seeded polymerization; and $K_t = K_{t_0}$ and $K_p = K_{p_0}$, respectively, before the gel effect took place.

Region II ($x_c \leq x \leq x_g$)

Once the monomer droplets disappeared, $[M]_p$ was no longer constant. The viscosity in the reaction zone became higher and higher with increasing conversion, the termination of polymer radicals became more difficult, and gel effect was significant. So, the rate constant of termination must be modified by the empirical equation

$$K_t = K_{t_0}T(x) \quad (14)$$

$$T(x) = \left(\frac{1 - x}{1 - x_c}\right)^2 \exp\{-2.7[(x - x_c) + (x - x_c)^2]\} \quad \text{(at 70°C)} \quad (15)$$

$$T(x) = \left(\frac{1 - x}{1 - x_c}\right)^2 \exp\{-4.5[(x - x_c) + (x - x_c)^2]\} \quad \text{(at 60°C)} \quad (16)$$

Also, $[M]_p$ dropped linearly with the conversion as seen in Figure 4, i.e.

$$[M]_p = [M]_s = [M]_g \frac{1 - x}{1 - x_c} \quad (17)$$

where x_c is the onset conversion at which monomer droplets disappeared, and $[M]_g$, the saturated monomer concentration in polymer particles.

By substituting eqs. (14)–(17) into eq. (9), we obtained

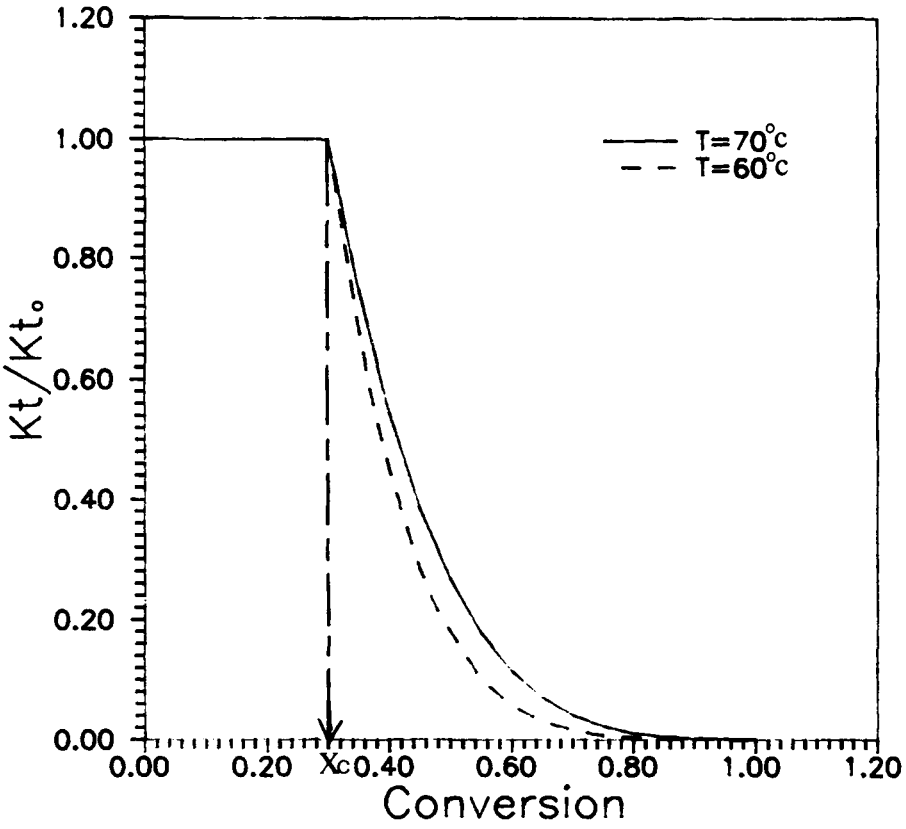

Figure 7 K_t/K_{t_0} vs. conversion.

$$[M]_0 \frac{dx}{dt} = K_{P_0}[M]_g \frac{1-x}{1-x_c}\left(\frac{\rho_i}{K_{t_0}T(x)}\right)^{1/2} \times \left(\frac{[M]_0 x \cdot 104}{\rho_p\left(1 - \frac{[M]_g(1-x)\cdot 104}{\rho_M(1-x_c)}\right)}\right)^{1/2} \quad (18)$$

Region III ($x_g \leq x < 1.0$)

In the latter period of reaction, the viscosity of the reaction mixture became very high. Even the propagation of monomers was significantly hindered, and the glassy effect was obvious. So, the rate constant of propagation (K_p) must be modified empirically as

$$K_p = K_{p_0}P(x) \quad (19)$$

$$P(x) = \exp(-4.3x) \quad \text{(at 70°C)} \quad (20)$$

$$P(x) = \exp(-5.2x) \quad \text{(at 60°C)} \quad (21)$$

Substituting eqs. (14)–(17) and (19)–(21) into eq. (9), we obtained

$$[M]_0 \frac{dx}{dt} = K_{P_0}[M]_g \frac{1-x}{1-x_c}\left(\frac{\rho_i}{K_{t_0}}\right)^{1/2} \times \frac{P(x)}{T(x)^{1/2}}\left(\frac{[M]_0 x \cdot 104}{\rho_p\left(1 - \frac{[M]_g(1-x)\cdot 104}{\rho_M(1-x_c)}\right)}\right)^{1/2} \quad (22)$$

The modified K_t and K_p in regions II and III to describe the gel effect and glassy effect were obtained from curve fitting. The modified terms in both K_t and K_p depended on the temperature and conversion, but were independent of the MMA/styrene ratios. It was reasonable that the modified term became less significant with increasing the temperature but became more significant with an increase of conversion.

Average Molecular Weight of Polymers

The core–shell polymer composite in this work contained PMMA polymer chains in the core and PS polymer chains in the shell. The average molecular weight of the polymers was calculated by the additivity rule as follows:

$$\overline{M}_{n_{(\text{mix})}} = \frac{N_{\text{PMMA}}\overline{M}_{n_{(\text{PMMA})}} + N_{\text{PS}}\overline{M}_{n_{(\text{PS})}}}{N_{\text{PMMA}} + N_{\text{PS}}} \quad (23)$$

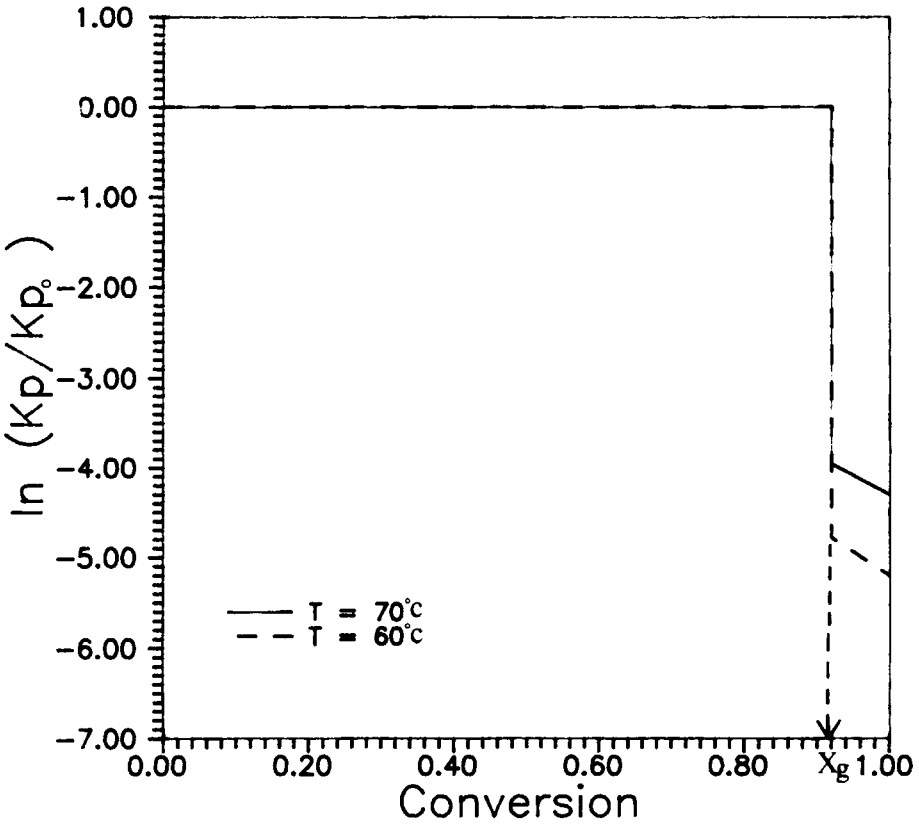

Figure 8 K_p/K_{P_0} vs. conversion.

where $\overline{M}_{n(\text{mix})}$ is the number-average molecular weight weight of the core–shell polymer composite; N_{PMMA}, the number of PMMA polymer chains; N_{PS}, the number of PS polymer chains; $\overline{M}_{n(\text{PMMA})}$, the number-average molecular weight of PMMA; and $\overline{M}_{n(\text{PS})}$, the number-average molecular weight of PS, or

Table I Parameter Used in the Simulation of Core–Shell Model

		T = 343°C	T = 333°C	References
$[M]_0$	mol/L-H_2O	0.932, 1.24	0.932, 1.24	Table 2 in Part I
K_{P_0}	L/min mol	$2.56 \cdot 10^4$	$1.63 \cdot 10^4$	Ref. 14
$K_{p_0}\left(\frac{\rho_i}{K_{t_0}}\right)^{1/2}$	$\frac{1}{\text{min}}\left(\frac{l}{l - H_2O}\right)^{1/2}$	$7.03 \cdot 10^{-3}$	$3.62 \cdot 10^{-3}$	From curve fitting
$\frac{(K_{t_0}\rho_i)^{1/2}}{K_{p_0}}$	$\left(\frac{1}{l - H_2O \cdot l}\right)^{1/2}$ mol	$2.15 \cdot 10^{-3}$	$1.2 \cdot 10^{-3}$	From curve fitting
ρ_P	g/L	1062	1062	Ref. 15
ρ_M	g/L	905	905	Ref. 15
$[M]g$	Mol/L	4.5	4	From Figure 4
X_c		0.3	0.3	From Figures 4 and 5
Gel effect (K_t)				From eqs. (14)–(16)
Glassy effect (K_p)				From eqs. (19)–(21)
M	g	73.77, 98.36	73.77, 98.36	Table 2 in Part I

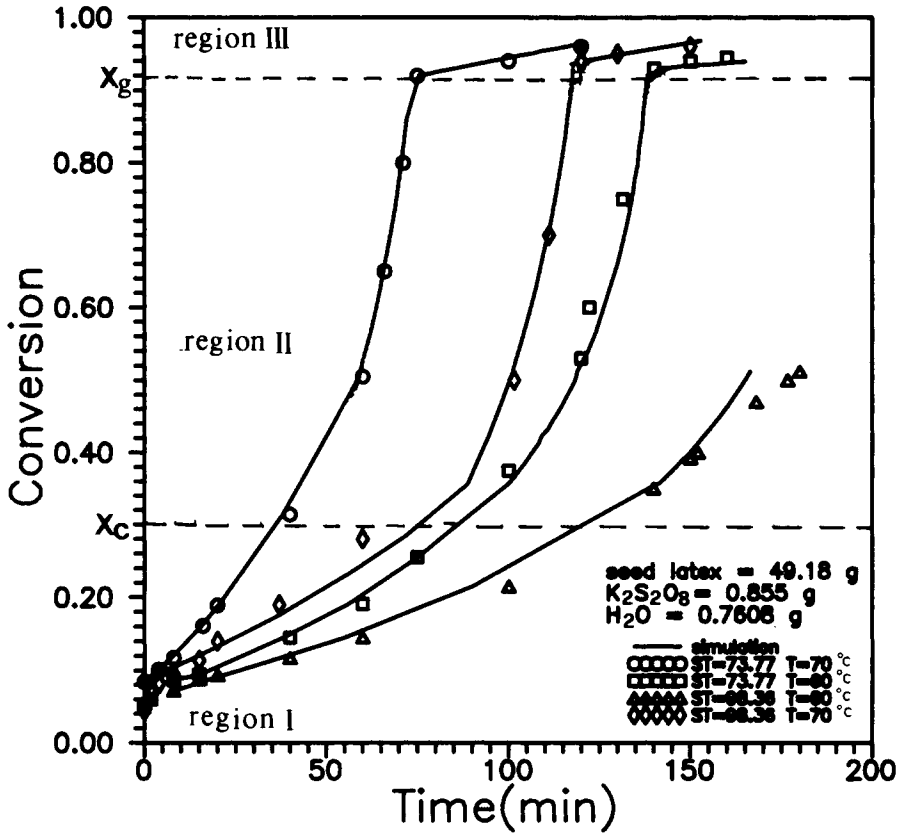

Figure 9 Conversion vs. reaction time; comparison of core–shell model simulation and experimental data.

$$\overline{M}_{n(\text{mix})} = \frac{W_{\text{PMMA}} + W_{\text{PS}}}{N_{\text{PMMA}} + N_{\text{PS}}} = \frac{W_{\text{PMMA}} + W_{\text{PS}}}{N_{\text{PMMA}} + \left(\dfrac{W_{\text{PS}}}{\overline{M}_{n(\text{PS})}}\right)} \tag{24}$$

where W_{PMMA} is the weight of PMMA, and W_{PS}, the weight of PS.

The number-average molecular weight of PS is calculated as follows:

$$\overline{M}_{n(\text{PS})} = \frac{x}{\displaystyle\int \frac{x}{\overline{M}_{n_i}}\,dx} = \frac{M_x}{\dfrac{1}{M}\displaystyle\int \frac{M_x}{\overline{M}_{n_i}}\,d(M_x)}$$

$$= \frac{W_{(\text{PS})}}{\dfrac{1}{M}\displaystyle\int \frac{W_{(\text{PS})}}{\overline{M}_{n_i}}\,dW_{(\text{PS})}} = \frac{MW_{(\text{PS})}}{\displaystyle\int \frac{W_{(\text{PS})}}{\overline{M}_{n_i}}\,dW_{(\text{PS})}} \tag{25}$$

where x is the conversion; M, the weight of styrene monomer fed into the system; and $\overline{M}_{n_i}$, the instantaneous number-average molecular weight of PS.

$\overline{M}_{n_i}$ was calculated from instantaneous kinetic chain length $\overline{X}_{n_i}$ as

$$\frac{\overline{M}_{n_i}}{104} = 2\overline{X}_{n_i} = 2\frac{R_p}{R_t}$$

$$= 2\frac{K_P[M]_s[R\cdot]V_rN}{K_t[R\cdot]^2V_rN} = 2\frac{K_P[M]_s}{K_t[R\cdot]} \tag{26}$$

where $[M]_s = [M]_p$ [eq. (2)] and the factor 2 in eq. (26) accounted for the recombination termination. Assuming a steady state for $(R\cdot)$, i.e., substituting eq. (5) into eq. (26), then

$$\frac{\overline{M}_{n_i}}{104} = 2\overline{X}_{n_i} = 2\frac{K_P[M]_p}{(K_t\rho_i)^{1/2}}V_r^{1/2}N^{1/2} \tag{27}$$

Introducing V_r of eq. (8) into eq. (27), we obtain

$$\overline{M}_{n_i} = 2 \times 104 \times \frac{K_p[M]_p}{(K_t\rho_i)^{1/2}} \frac{W_p^{1/2}}{\left(\rho_p\left(1 - \dfrac{[M]_p \cdot 104}{\rho_M}\right)\right)^{1/2}} \tag{28}$$

Substituting eqs. (25) and (28) into eq. (24), we obtain

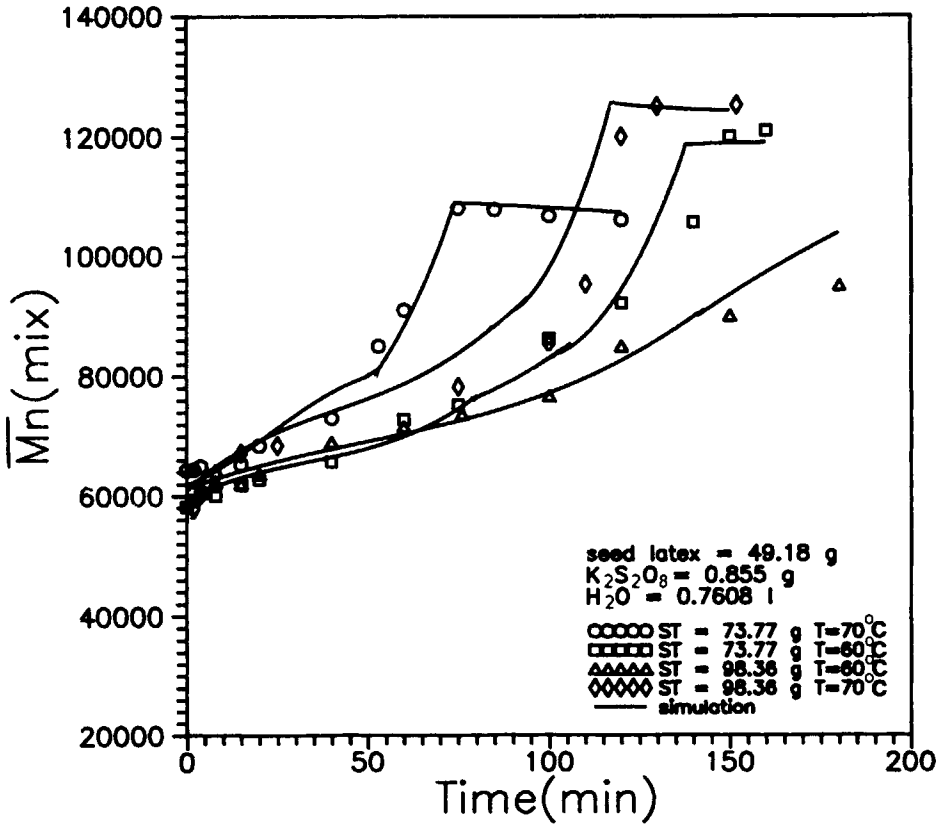

Figure 10 Number-average molecular weight of polymer composite [$M_{n_{(mix)}}$] vs. reaction time; comparison of core–shell model simulation and experimental data.

$$\overline{M}_{n_{(mix)}} = \frac{W_{PMMA} + W_{PS}}{N_{PMMA} + \frac{1}{M}\int \frac{(K_t\rho_i\rho_p)^{1/2}\left(1 - \frac{[M]_p \cdot 104}{\rho_M}\right)^{1/2}(0.7608)^{1/2}}{W_{PS}^{1/2} \times 2 \times 104 \times K_p[M]_p} dW_{PS}} \tag{29}$$

where $W_{PS} = M \cdot X$.

Equation (29) is available for three regions of polymerization. The important features for three regions are summarized as

(1) Region I
$[M]_p$ = constant.
$K_t = K_{t_0}$ = constant.
$K_p = K_{p_0}$ = constant.

(2) Region II
$[M]_p$ decreased linearly with increasing conversion as eq. (17).
K_t decreased with increasing conversion as eqs. (14), (15), and (16).
$K_p = K_{p_0}$ = constant.

(3) Region III
$[M]_p$ decreased linearly with increasing conversion as eq. (17).
K_t decreased with increasing conversion as eqs. (14)–(16).
K_p decreased with increasing conversion as eqs. (19)–(21).

RESULTS AND DISCUSSION

Morphology

With PMMA latex as the seeds and $K_2S_2O_8$ as the initiator, styrene was polymerized by the method of seeded soapless emulsion polymerization, which formed the PMMA/PS composite latex. The morphology of the PMMA/PS composite latex was with a core–shell structure as seen in Figure 2.

To examine the concentration profile of styrene in the PMMA seed latex particle in the seeded po-

lymerization, the water-soluble initiator ($K_2S_2O_8$) was replaced by an oil-soluble initiator (AIBN) during the seeded polymerization. In the first stage, we obtained the PMMA seed latex as before, next the PMMA seed latex was swollen with the mixing solution of styrene and AIBN for 24 h at room temperature, and then the reaction of polymerization proceeded at 70°C. After the reaction was complete, the composite latex particle was sectioned, stained, and observed under the TEM. The morphology of the composite latex particle with AIBN as the initiator showed that PS was distributed uniformly in the composite particle as in Figure 3, from which it was indicated that the PMMA seed latex was rather uniformly swollen with styrene in the seeded polymerization.

Concentration of Monomer in Polymer Particles ($[M]_p$)

The relation between conversion and concentration of monomer in polymer particles was observed from experiments. The result is shown in Figure 4. In the earlier period of reaction, monomer droplets still existed in the system; the concentration of the monomer in the polymer particles was kept at a constant value ($[M]_g$). It meant that the monomers diffused from monomer droplets into the polymer particles very quickly during the reaction whenever monomer droplets existed in the reaction system, so the concentration of the monomer in the polymer particles was retained at a saturated concentration. After the monomer droplets disappeared, the concentration of the monomer in the polymer particles was unable to retain the saturated concentration; it would decrease linearly with increasing conversion. The value of $[M]_g$ was about 4.5 mol/L at 70°C and 4 mol/L at 60°C.

Determination of the Onset Conversion (x_c) When the Monomer Droplets Disappeared

To determine the onset conversion (x_c) when the monomer droplets disappeared, the mass balance eq. (30) was used to calculate the weight of monomer droplets that existed in the reaction system. The equation is stated as

$$V \cdot [M]_p \cdot N \cdot 0.7608 \cdot 104 + X \cdot M + md = M \quad (30)$$

where the factor 0.7608 is the volume (liter) of water fed into the reaction system; V, the average volume of polymer particles which could be calculated from the diameter of the latex particle (the data were shown in the Part I of our work, Fig. 3); and md, the weight of monomer droplets that existed in the reaction system.

Figure 5 shows the plots of conversion vs. the weight of monomer droplets at different MMA/ST weight ratios and different temperatures. It appeared that the monomer droplets disappeared approximately at a conversion of 0.3. Another indication was that the monomer concentration in polymer particles began to decrease at a conversion of about 0.3, as shown in Figure 2. So, we set the onset conversion (x_c) as 0.3 in the calculation of the model for simplicity.

Polymer Yield

Figure 6 shows the experimental data of 0.5 power of the PS yield vs. reaction time in the earlier period of the reaction at different MMA/ST monomer weight ratios and different temperatures in seeded polymerization. It shows that the reaction time was proportional to the 0.5 power of the PS yield. The slope of the line was higher at higher temperature, but independent of the MMA/ST ratio. This finding agreed with the relation of the polymer yield to reaction time in the core–shell model stated in eq. (13).

Additionally, in Part I of our work, it was found that the slope of the line of $(W_p)^{1/2}$ vs. time was proportional to the 0.5 power of the initiator concentration, but independent of the seed content, which could all be predicted from eq. (13). As the gel effect became important, i.e., the viscosity of the system in the reaction zone became higher in region II, the termination of polymer radicals became more difficult. So, the rate constant of termination must be modified by empirical eqs. (14)–(16). The results showed that an increase of conversion would decrease k_t as shown in Figure 7. Similarly, when the glassy effect took place in region III, the propagation rate constant (k_p) would decrease with increasing conversion, as shown in Figure 8 and eqs. (19)–(21).

In the calculation of eqs. (12), (18), and (22) of the core–shell model, $[M]_p$ was determined from eq. (17), together with all the parameters in Table I. The kinetic simulation of conversion by the core–shell model and the experimental data are shown in Figure 9. The results showed that the conversion prediction by the core–shell kinetic model fitted well with the experimental data. The increases of temperature and the MMA/ST weight ratio would increase the rate of polymerization.

Number-average Molecular Weight of Polymers

Equation (29) was used to calculate the number-average molecular weight of the polymers in our

core–shell model. W_{PMMA} and N_{PMMA} were obtained as 49.18 g and 8.9×10^{-4} mol, respectively, from the seed emulsion in the first stage of the reaction. The other parameters are listed in Table I for the calculation. Figure 10 shows the prediction of $\overline{M}_{n(mix)}$ of eq. (29) and the experimental data. The results showed that the prediction by the core–shell kinetic model conformed well with the experimental data.

Parameters $K_{p_0}(\rho_i/K_{t_0})^{1/2}$ and $[(K_{t_0}\rho_i)^{1/2}/K_{p_0}]$

The value of $K_{p_0}\left(\frac{\rho_i}{K_{t_0}}\right)^{1/2}$ was obtained from the slope of the line of $(W_p)^{1/2}$ vs. time in Figure 6. It was 7.03×10^{-3} (1/min)$[1/(1 - H_2O)]^{1/2}$ at 70°C and 3.62×10^{-3} (1/min)$[l/(l - H_2O)]^{1/2}$ at 60°C, respectively.

The value of $[(K_{t_0} \cdot \rho_i)^{1/2}]/K_{p_0}$ was obtained by the curve fitting of $\overline{M}_{n(mix)}$ vs. time in Figure 10. It was 2.15×10^{-3} $[1/(1 - H_2O \cdot 1)]^{1/2}$ mol at 70°C and 1.2×10^{-3} $[1/(1 - H_2O \cdot 1)]^{1/2}$ mole at 60°C, respectively.

Substituting the value of k_{p_0} (Ref. 14) into $K_{p_0}(\rho_i/K_{t_0})^{1/2}$ and $\{[(K_{t_0} \cdot \rho_i)^{1/2}]/K_{p_0}\}$, we obtained the values of ρ_i and k_{t_0} as 1.51×10^{-5} [mol/(min 1 − H_2O)], 2×10^8 [1/(mol min)] at 70°C and 4.34×10^{-6} [mol/(min 1 − H_2O)], 8.76×10^7 [1/(mol min)] at 60°C, respectively.

Here, the initiator concentration was calculated as $[I] = 1.73 \times 10^{-3}$ mol/L (from seed latex) + 2.43×10^{-3} mol/L (from the second stage of the reaction). So, the value of fk_d could be obtained from eq. (10) as

$$fK_d = \frac{\rho_i}{2[I]}$$

The value of fk_d was 1.81×10^{-3} L/min and 5.22×10^{-4} L/min at 70 and 60°C, respectively. Some literature reported the value of k_d as 1.61×10^{-3} L/min at 70°C (Ref. 14) and 1.9×10^{-4} L/min at 60°C (Ref. 14), so the values of fk_d obtained from our model are quite reasonable. The value of k_{t_0} in Ref. 16 was 1.32×10^8 L/min mol at 70°C, which was also close to our prediction of k_{t_0}.

CONCLUSION

The morphology of PMMA/PS composite latex particles synthesized by two-stage soapless emulsion polymerization (i.e., seeded emulsion polymerization) with $K_2S_2O_8$ as the initiator was with a core–shell structure. A core–shell model was proposed. The model divided the course of polymerization into three regions: Monomer droplets existed in region I, the gel effect was taken into account in region II, and the glassy effect was considered in region III.

The termination rate constant and propagation rate constant were modified by empirical equations, respectively, for the gel effect and the glassy effect. The prediction of the conversion and the number-average molecular weight of polymers during the seeded emulsion polymerization on the basis of our core–shell kinetic model fit well with the experimental data. Reasonable values of the termination rate constant (k_{t_0}) and the initiation rate constant (fk_d) were obtained by fitting the experimental data to our core–shell model.

NOMENCLATURE

f	initiator efficiency
$[I]$	initiator concentration (mol/L-H_2O)
K_d	rate constant for initiator decomposition (L/min)
K_{p_0}	propagation rate constant before gel effect took place (L/min mol)
K_p	propagation rate constant (L/min mol)
K_{t_0}	termination rate constant before gel effect took place (L/min mol)
K_t	termination rate constant (L/min mol)
M	weight of styrene monomer fed into the reaction system (g)
$[M]_0$	initial monomer concentration (mol/L-H_2O)
$[M]_c$	monomer concentration in the core (mol/L)
md	weight of monomer droplets in the reaction system (g)
$[M]_g$	saturated monomer concentration in the polymer particle (mol/L)
$\overline{M}_{n_i}$	instantaneous number-average molecular weight of PS (g/mol)
$\overline{M}_{n(mix)}$	number-average molecular weight of the core–shell polymer composite (g/mol)
$\overline{M}_{n(PMMA)}$	number-average molecular weight of PMMA (g/mol)
$\overline{M}_{n(PS)}$	number-average molecular weight of PS (g/mol)
$[M]_p$	monomer concentration in polymer particle (mol/L)
$[M]_s$	monomer concentration in shell (mol/L)
N	particle number per unit volume of water (L/L-H_2O)
N_{PMMA}	number of PMMA polymer chains (mol)
N_{PS}	number of PS polymer chains (mol)
R_p	rate of polymerization (mol/min L/H_2O)
t	reaction time (min)
V	average volume of polymer particles (L)

V_r	volume of reaction zone (L)
W_p	PS yield in seeded polymerization per liter water (g/L-H_2O)
W_{p_0}	PS yield initially in seeded polymerization per liter water (g/L-H_2O)
W_{PS}	weight of PS (g)
W_{PMMA}	weight of PMMA (g)
X	conversion
X_c	the onset conversion when the monomer droplets disappeared
X_g	the onset conversion when the glassy effect took place
$\overline{X_{n_i}}$	instantaneous kinetic chain length
ρ_i	generation rate of free radicals (mol/min L-H_2O)
ρ_m	density of styrene (st) (g/L)
ρ_p	density of polystyrene (PS) (g/L)
$\overline{\rho_p}$	average density of PMMA and PS (g/L)

REFERENCES

1. C. F. Lee, K. R. Lin, and W. Y. Chiu, *J. Appl. Polym. Sci.*, **56,** 1263 (1995).
2. M. S. Silverstein, Y. Talmon, and M. Narkis, *Polymer,* **30,** 416 (1989).
3. S. Lee and A. Rudin, *J. Polym. Sci. Polym. Chem. Ed.,* **30,** 2211 (1992).
4. D. G. Cook, A. Rudin, and A. Plumtree, *J. Appl. Polym. Sci.,* **46,** 1387 (1992).
5. S. Muroi, H. Hashimoto, and K. Hosoi, *J. Polym. Sci. Polym. Chem. Ed.,* **22,** 1365 (1984).
6. D. I. Lee and T. Ishikawa, *J. Polym. Sci. Polym. Chem. Ed.,* **21,** 147 (1983).
7. T. I. Min, A. Klein, M. S. El-Aasser, and J. W. Vanderhoff, *J. Polym. Sci. Polym. Chem. Ed.,* **21,** 2845 (1983).
8. M. R. Grancio and D. J. Williams, *J. Polym. Sci. Parts A-1,* **8,** 2617 (1970).
9. R. A. Wessling and I. R. Harrison, *J. Polym. Sci. Part A-1,* **9,** 3471 (1971).
10. J. Ugelstad and F. K. Hansen, *Rubber Chem. Tech.,* **49,** 536 (1976).
11. J. L. Gardon, *Br. Polym. J.,* **1,** 1 (1979).
12. W. Y. Chiu, S. M. Lai, L. W. Chen, and C. C. Chen, *J. Appl. Polym. Sci.,* **42,** 2787 (1991).
13. H. F. Mark, N. M. Bikales, N. G. Gaylord et al., *Encyclopedia of Polymer Science and Technology,* Wiley, New York, 1976.
14. Z. Song and G. W. Poehlein, *J. Polym. Sci. Polym. Chem. Ed.,* **28,** 2359 (1990).
15. J. Brandrup and E. H. Immergut, *Polymer Handbook,* Wiley-Interscience, New York, 1975.
16. A. W. Hui and A. E. Hamielec, *J. Appl. Polym. Sci.,* **10,** 749 (1972).

Received October 15, 1993
Accepted January 22, 1995